International Journal of Sciences

Research Article Volume 3 - April 2014 (4)

Low-Temperature Hydrothermal Synthesis of Zinc Oxide Structures on Glass, Silicon and Indium Tin Oxide Substrates

Gérrard Eddy Jai Poinern[1], Derek Fawcett[1]

[1]Murdoch Applied Nanotechnology Research Group, Department of Physics, Energy Studies and Nanotechnology School of Engineering and Energy, Murdoch University, Murdoch, Western Australia 6150, Australia, Fax: +61 8 9360-6183

Abstract: In this study, a low-temperature hydrothermal method is used to synthesize crystalline zinc oxide powders with various morphologies on glass, silicon and indium tin oxide substrates. The study found that each respective substrate produced a variation in the morphology of the zinc oxides produced at the reaction temperature of 90 ºC. The crystallinity and particle size of the zinc oxide structures on each substrate type was characterized using both X-ray diffraction and Field Emission Scanning Electron Microscopy.

1. Introduction

Nanometre scale zinc oxide (ZnO) is an extremely significant semiconductor material due to its unique properties and its wide range of morphologies. The lack of a centre of symmetry in the hexagonal wurtzite form, combined with a number of favourable properties such as a wide band gap of 3.37 eV, a high exciton binding energy of 60 meV at room temperature, high electron mobility, catalytic and electronic properties have made ZnO an attractive material for a variety of electronics, photonic and various optoelectronic applications [1-7]. In addition, ZnO has been found to be a biological compatible material, which has been used in a number of potential biomedical applications such as selectively destroying tumor cells and drug delivery applications [8-10]. In recent years, studies into one dimensional (1-D) and the more complex three dimensional (3-D) nanometre scale structures have attracted a great deal of interest due to the potential applications in optoelectronics [11], transistors [12, 13], flat panel displays [14], dye sensitized solar cells [15, 16], conductive films [17, 18] and sensors [19-25]. This diverse range of potential technological based applications clearly demonstrates the importance ZnO will play in the future development of new devices and sensors. In order to fully exploit ZnO for these potential applications, it is important to develop simple and efficient synthesis methods to control the crystal size, crystalline density and morphology of the nanometre and micrometre scale structures needed to produce the desired material properties [24].

In particular, some studies have shown that the morphology has a significant role in determining the final material properties of the synthesized ZnO. Consequently, a diverse range of synthesis techniques have been developed to produce a wide range of morphologies both in the micrometre and nanometre scale. Nanometre scale morphologies such as nano-wires [26], nano-rods [27], nano-tubes [28], nano-plates [29] and nano-helices [30] have been studied, while micrometre scale structures such as micro-boxes [25], micro-cheerios [24], micro-combs [26] and micro-flowers [27] have also been extensively investigated.

To date, a large variety of ZnO structures, both at the nanometre and micrometre scale have been fabricated using a diverse range of different synthesis techniques [31-34]. Techniques such as chemical vapour deposition [35, 36], thermal evaporation [33], vapour liquid solid growth [37] and vapour phase deposition [38-40] have been successfully used to produce ZnO structures. However, the operational costs of these techniques are relatively high in some cases due to the complex and expensive equipment used and synthesis procedures that require high temperatures (up to 1400ºC). Alternative fabrication techniques using solution based chemical synthesis has the advantages of lower process temperatures, straight-forward operation and the potential of scaling up production due to their inherent low cost and efficiency. Conversely, there are often much longer synthesis times involved in solution based chemical growth techniques and there is also a reduction in the control of the resulting morphology [41]. Typical solution based techniques that have been used to produce a wide variety of ZnO structures with different shapes and dimensions include sol-gel [42], template assisted growth [43, 44] and hydrothermal methods [45-47].

Gérrard Eddy Jai Poinern (Correspondence)
g.poinern@murdoch.edu.au
+61 8 9360-2892

In this article we present a new low-temperature hydrothermal method that synthesizes a variety of 1-D and 3-D ZnO structures, both at the nanometre and micrometre scales on glass, silicon and indium tin oxide substrates. The first advantage of using this technique is that it uses standard laboratory equipment such as a hotplate fitted with a magnetic stirrer and glassware. The second advantage of this technique is the low synthesis temperature of 90 ºC which is capable of producing a range of ZnO structures within 60 minutes. Field emission scanning electron microscopy (FESEM) was used to examine the various ZnO structures formed the substrates and the effect of substrate material on growth and morphology of the resulting nanometre and micrometre scale structures. In addition, X-ray diffraction (XRD) was used to confirm the crystalline structure of the synthesized ZnO structures. The hydrothermal technique produced a number of different morphologies on the same substrate, which indicated the chaotic nature of the solution-based method and the inherent difficulty of controlling the crystal growth.

2. Materials and methods

2.1. Materials

Analytical reagent grade Zinc sulfate heptahydrate [$ZnSO_4.7H_2O$] (Batch No 227571) and ammonium chloride [NH_4Cl] (Batch No 235861) were supplied by Chem Supply Pty Ltd. Analytical reagent grade Urea [CH_4N_2O] (Batch No AF602137) was obtained from Ajax Fine Chem. The ammonia solution used was analytical reagent grade (28% w/w, Batch No 234228) and was supplied by Bio Lab. The substrates used in these studies consisted of glass microscope slides (Sail, Australia), Esco glass cover slips (Bio-lab Ltd), Silicon chip wafers (Pro SciTech, Australia) and indium tin oxide glass slides (Delta Technologies Ltd, USA). Milli-Q® water (18.3 MΩ cm^{-1}) was used in all aqueous solution preparations and was produced from a Barnstead Ultrapure Water System D11931 (Thermo Scientific, Dubuque, IA).

2.2. Preparation of substrates and stock solution

2.2.1. Substrate preparation

The substrates used in this study consisted of glass microscope sides and glass cover slips, indium tin oxide glass slides and silicon chip wafers. The cleaning procedure consisted of a two-step procedure. In the first step all substrate types were individually placed in a 15 mL solution of reagent grade ethanol and then subjected to 15 minutes of low power ultrasound irradiation using an Transtek® Systems Soniclean 30A (20 W) at a room temperature of 24 °C. This procedure was carried out 3 times, each time a fresh quantity of ethanol was used. At the end of the ethanol/ultrasound treatment the substrates were individually rinsed in Milli-Q® water ready for the next step. During the second step the substrates were individually placed into a 50 mL solution of Milli-Q® water and subjected to another 3 ultrasound treatments each lasting 15 minutes. Fresh Milli-Q® water was used for each treatment. At the end of the two-step cleaning procedure all substrates were left to soak in fresh Milli-Q® water for 24 hours and then stored for future.

2.2.2. Preparation of stock solution of reactants

A stock solution composed of 25 mL of 0.01 mol l^{-1} of urea, 200 mL of 0.01 mol L^{-1} of zinc sulphate heptahydrate and 25 mL of ammonia solution (28% w/w) were added to 250 mL solution of 0.02 mol L^{-1} ammonium chloride contained in a glass vessel. The glass vessel was then sealed and then the solution was slowly mixed for 30 minutes. At the end of the initial mixing stage, the heating cycle was initiated and the solution was slowly heated up to 90 ºC. After thermal equilibrium had been achieved the substrates were placed into the sample holder, which was then placed into the glass vessel, as schematically presented in Figure 1. During the next 90 minutes, substrates were removed from the solution at 5, 10, 15, 20, 30, 45, 60 and 90 minute time intervals. The individual substrates were rinsed using Milli-Q® water and air dried ready for characterization.

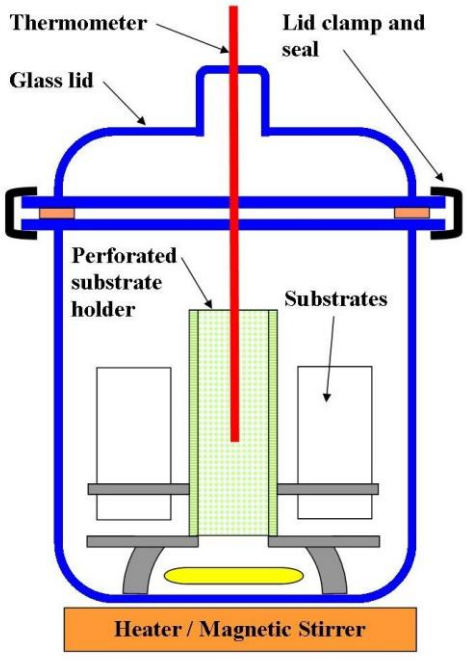

Figure 1 Schematic of glass vessel assembly used in the low temperature hydrothermal process.

2.3. Characterization of substrates

The products deposited on the respective substrates were characterized by X-ray diffraction spectroscopy (XRD) and Field Emission Scanning Electron Microscopy (FESEM). XRD was used to verify the formation and identify compounds present on the

respective substrate surfaces using a Siemens D500 series diffractometer [Cu K_α = 1.5406 Å radiation source] operating at 40 kV and 30 mA, with an acquisition time of 2 seconds. The diffraction patterns were collected over a 2θ range from 20° to 45° with an incremental step size of 0.04° using flat plane geometry. The particle size and morphology were examined using FESEM. All micrographs were taken using a high resolution Zeiss 1555 VP-FESEM at 3 kV with a 30 µm aperture operating under a pressure of 1×10^{-10} Torr (Carl Zeiss, Oberkochen, Germany) located at the UWA Centre of microscopy and microanalysis. Samples were mounted on individual substrate holders using carbon adhesive tape before being coated with a 40 nm layer of gold to prevent charge build up during FESEM using a Cressington 208HR High Resolution Sputter coater.

3. Results and discussions

XRD spectroscopy was used to characterize the respective white precipitates found on each respective substrate type. All XRD patterns clearly indicated the presence of ZnO which was indexed as the hexagonal wurtzite structures (hexagonal phase, space group P63mc) according to JCPDS file card number 36-1451. XRD patterns for the 30 min and 60 min immersion periods are presented in this study since they were a good representation of the results produced using this low temperature hydrothermal method. A typical diffraction pattern for a glass microscope slide is presented in Figure 2 (a) with both the 30 min and 60 min immersion periods shown. The 30 min immersion pattern shows no ZnO peaks and corresponds to precursor type growth which is seen in the FESEM micrographs presented in Figure 3. The 60 min pattern shows sharp ZnO diffraction peaks corresponding to Miller indices (100), (002) and (101) which are located at 2θ positions of 31.82°, 34.54° and 36.38°, respectively. The sharp peaks indicate good crystallization of the ZnO structures in spite of the low temperature of the synthesis process, while the different peak intensities correspond to preferential growth planes in the forming oxide structures. XRD patterns for the Esco glass cover slips are not presented since they correspond to the glass microscope slide XRD data.

Typical XRD diffraction patterns of as-prepared ZnO powders on an indium tin oxide (ITO) glass slide substrate are present in Figure 2 (b). As in the case of the glass microscope slide, the 30 min immersion pattern with only precursor growth showed no ZnO peaks. However, the XRD pattern for 60 min immersion revealed five sharp peaks. The three ZnO peaks (100), (002) and (101) were again present, with the only difference being in their respective intensities. For example, in the case of the glass microscope slide the (002) peak intensity was 3.7 times great than the intensities for the (101) and (100) peaks. While for the ITO substrate the (002) peak intensity was only 1.1 times greater than the (101) peak and 1.3 times greater than the (100) peak. The difference in peak intensities seen in the ITO substrate indicates that there is a difference in the preferential growth planes than those seen in the microscope slides. In addition, there are also two extra ITO related peaks centred on 30º and 35º of the 2θ axis which correspond to the (121) and (212) Miller indices assigned to ITO. From an XRD analysis point of view, the ZnO structures grown on the silicon chip wafers proved difficult to present. The three ZnO peaks seen in the XRD analysis for glass cover slips, microscope slides and ITO substrates were present on the silicon substrates, but due to the extremely large silicon peak they were difficult to see and as a result the XRD pattern is not present. The XRD analysis for the silicon substrate reveals that the (002) peak intensity is the largest and is 4.4 times greater than both the (100) and (101) intensities.

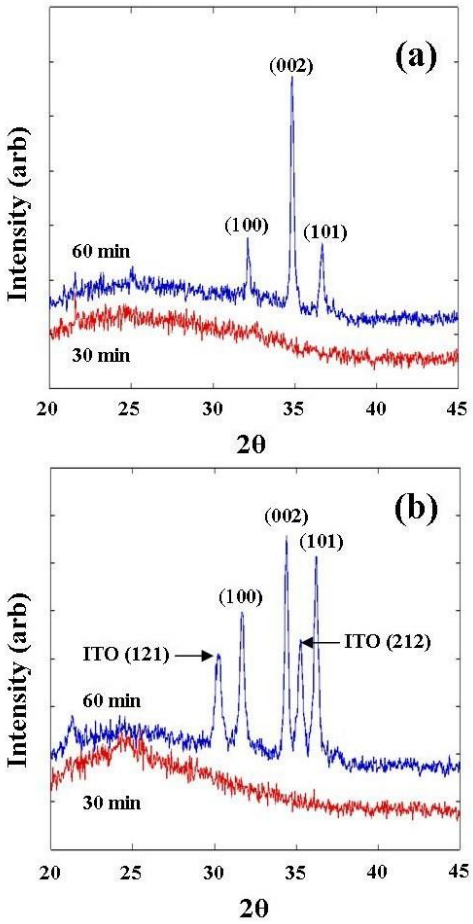

Figure 2 Typical XRD diffraction patterns of ZnO powders hydrothermally prepared at 90 ºC on (a) glass microscope slides and (b) indium tin oxide glass slides

The morphology of the various ZnO nanometre and

micrometre scale structures formed on different substrates during the low temperature hydrothermal method was investigated using FESEM. In this article only FESEM micrographs of the 30 and 60 minute growth periods are presented since they are representative of the typical ZnO structures formed during the time-growth study. There was extensive surface coverage of ZnO structures on all substrates, but the structure size, shape and orientation varied considerably. In the case of the Esco glass cover slips, the growth after 30 minutes was dense and consisted of unaligned hexagonal rods which appear to be growing randomly over the substrate surface as seen in Figure 3 (a). The rods were found to have a fairly uniform diameter of 150 nm, while their length ranged from 0.5 to 1.2 µm. Greater immersion times, hence longer growth periods tended to produce much larger rod diameters and lengths. The micrograph presented in Figure 3 (b), taken after 60 minutes of immersion confirms this growth. Examination of the images revealed that the diameter of the rods ranged from 200 to 500 nm; while their length ranged from 0.7 to 3.5 µm (aspect ratio ranges from 3.5 to 7). In addition, two new features were seen that were not seen on substrates from the 30 minute immersion period. The first feature consisted of regions of densely packed, vertically aligned rods that appeared to grow directly up from the surface as seen in the blue box in Figure 3 (b). The diameter of the vertical hexagonal rods was found to range from 200 to 300 nm, while the length ranged from 0.8 to 2.0 µm (aspect ratio ranges from 4 to 6.7). The second feature consisted of clusters that resembled flower-like micrometre scale structures which were constructed of numerous rods. The rods had diameters ranging from 500 to 900 nm, while the length of the rods ranged from 3.0 to 4.5 µm (aspect ratio ~ 6).

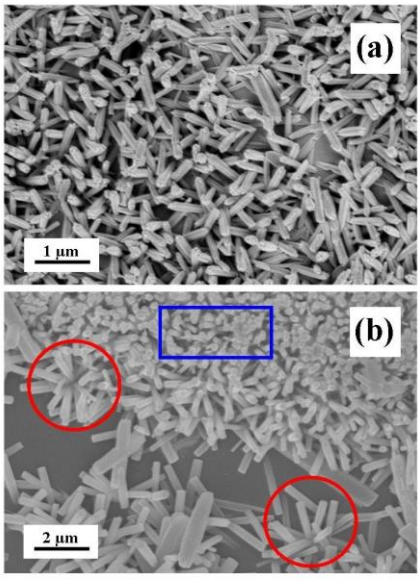

Figure 3 Typical FESEM micrographs of ZnO powder prepared on Esco glass cover slips: (a) 30 min growth period and (b) 60 minute growth period.

The second substrate examined was the glass microscope slide and like the glass cover slip, the ZnO formations were similar for the 30 minute immersion and growth period. The microscope slide was found to have an underlying layer of unaligned hexagonal rods which appear to be randomly covering the surface. Examination of the images revealed that the diameter of the rods ranged from 100 to 200 nm and their length ranges from 0.6 to 1.0 µm (aspect ratio ~ 5). In addition to the carpet of rods are numerous regions of densely packed, vertically aligned rods that appeared to grow directly up from the surface with similar dimensions to the unaligned rods as seen in the blue box in Figure 4 (a). The vertical alignment found on the microscope slides was far more pounced than similar alignments found on the glass cover slips. Also present in small numbers are flower-like nanometre scale structures which are constructed of numerous rods which are typically 100 nm in diameter and 500 nm in length. The flower-like structures are highlighted in Figure 4 (a) by red circles. Besides the micrometre scale rods there are also numerous nanometre scales rods present in the ZnO. These rods were found to have a fairly uniform diameter of 50 nm, while their length ranged from 0.3 to 0.5 µm and are indicated by the yellow arrows in Figure 4 (b).

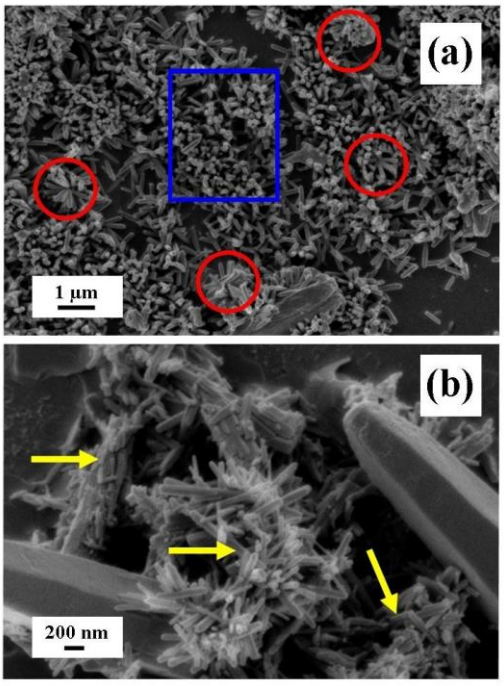

Figure 4 Typical FESEM micrographs of ZnO powder prepared on glass microscope slide slips after a 30 min growth period: (a) Landscape view of ZnO structures and (b) an enlarged view of nanometre scale rods

After a 60 minute growth period the surface structures on the microscope slide have become more pronounced. There are extensive regions of vertically aligned hexagonal rods with diameters ranging from 200 to 500 nm and lengths ranging from 3.0 to 5.5 µm. These vertical aligned regions are characterized by densely packed rods as seen in Figure 5 (a). Figure 5 (a) clearly shows the strong hexagonal crystalline growth that has taken place. However, between these densely packed regions are less dense regions of coral-like structures as seen in Figure 5 (b). The coral structures are characterized by micrometre scale flower-like structures that can be as large as 7 µm in diameter (highlighted by yellow circle in Figure 5 (b)). All of these flower-like structures are composed of numerous hexagonal rods growing out of a common growth centre. These structures range from the nanometre scale well into the micrometre scale as seen in Figure 5 (c). With the diameters of the hexagonal rods ranging from 200 nm up 1 µm, while their lengths range from 1.8 to 4.0 µm.

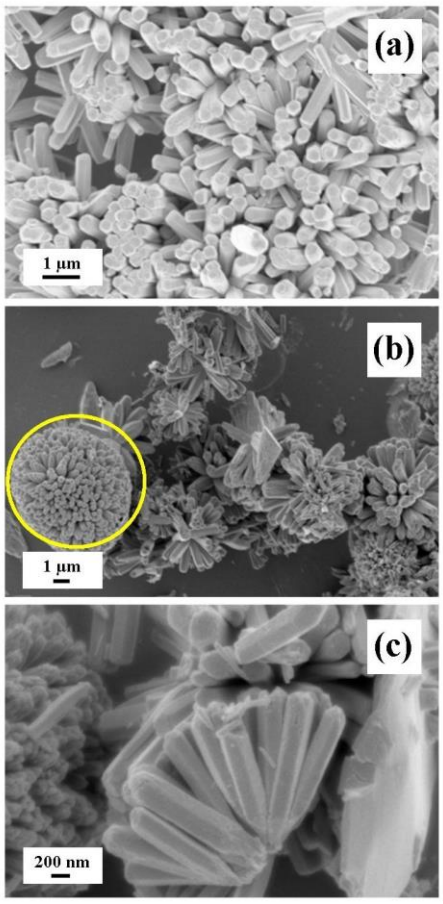

Figure 5 Typical FESEM micrographs of ZnO powder prepared on glass microscope slide slips after a 60 min growth period: (a) densely packed vertically aligned hexagonal rods; (b) less dense regions have coral-like structures, and (c) flower-like nanometre scale structures.

For the silicon substrate, the 30 minute growth period only produced nanometre scale spherical precursor structures that were typically 200 nm in diameter as seen in Figure 6 (a). These spherical precursor structures tended to be clumped together over the entire surface. However, the 60 minute period substrates showed a dramatic increase in ZnO growth. The spherical precursor structures were no longer present; instead three new types of oxide structure had grown on the substrate. The first structure consisted of hexagonal rods with diameters ranging from 200 to 800 nm and length ranging from 1 to 5 µm. Figure 6 (b) presents a typical rod highlighted in the blue box, its diameter was estimated to be 700 nm and has a length was found to be 4.3 µm, which gives it an aspect ratio of around 6. The second present was flower-like micrometre scale structures which are constructed of numerous rods which are typically around 300 nm in diameter and between 1 and 4 µm in length. The flower-like structures are highlighted in Figure 6 (b) by red circles. The third type of structure present on the silicon substrate was a fern like feature that was composed of numerous nanometre scale rods that were typically 100 nm in diameter and around 1 µm in length. The fern structure was only seen on the silicon substrate and is pointed out in Figure 6 (b) by the yellow arrows.

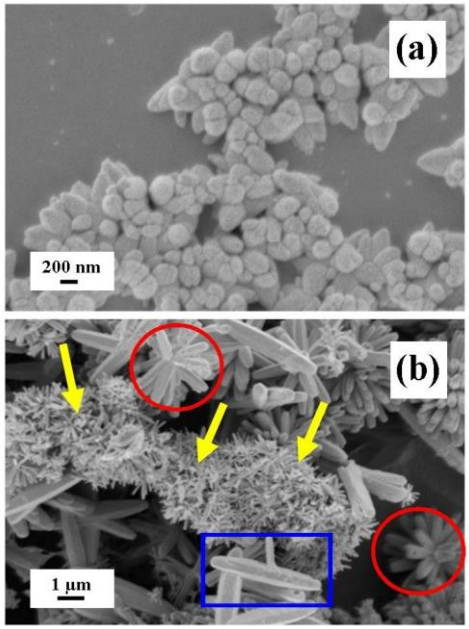

Figure 6 Typical FESEM micrographs of ZnO powder prepared on Silicon chip wafers: (a) precursor oxide growth after 30 minutes and (b) hexagonal rods (blue box), flower-like micrometre scale structures (red circles) and fern-like nanometre scale structures (yellow arrows).

Like the silicon substrate, the ITO substrate the initial

growth rate appeared slow compared to the glass substrates. The 30 minute growth period sample revealed only small spherical seeds approximately 200 nm in diameter. However, the 60 minute showed much more pronounced growth with numerous unaligned rods which appear to be randomly arranged over the substrate surface as seen in Figure 7 (a). The rods were found to have a diameter ranging from 300 to 500 nm, while their length ranged from 1.0 to 3.5 µm. In addition to the horizontal rods were a small number flower-like micrometre scale structures constructed of numerous rods. The rods in these structures were found to have diameters ranging from 200 to 300 nm and lengths between 2.0 and 2.5 µm (highlighted by red circle in Figure 7 (a)). The final feature seen on the ITO substrates was small islands of vertically aligned rods with diameters at the tips of around 200 nm as seen in Figure 7 (b). From the tips down towards the substrate surface the rod diameter steadily increases up to around 600 nm, while the lengths were estimated to be between 2.0 to 3.5 µm.

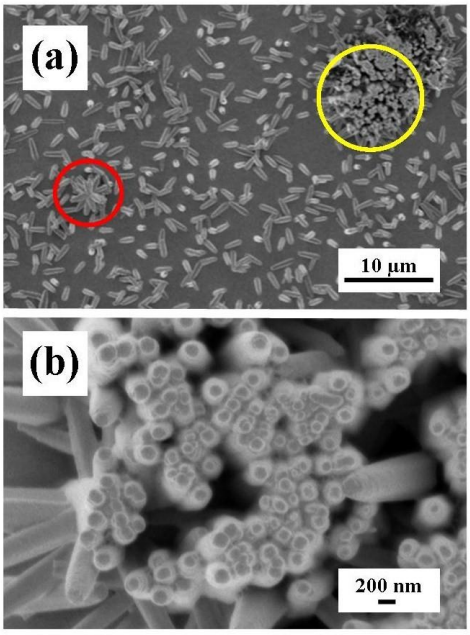

Figure 7 Typical FESEM micrographs of ZnO powder synthesized on ITO glass slides after a 60 minutes growth period.
(a) Numerous unaligned rods scattered over the surface; red circle indicates micrometre scale flower-like structure and yellow circle indicates a small island of vertically aligned rods.
(b) Enlargement of yellow circle showing tip geometry.

The results of this preliminary study indicate that it was possible to use a low-temperature hydrothermal method to produce a variety of nanometre and micrometre scale ZnO structures with different morphologies on glass, silicon and ITO substrates. The advantage of the low-temperature approach is that it has relatively low cost equipment, does not require low pressures or high temperatures, has easily controllable experimental parameters and can be easily scaled up to produce larger quantities of ZnO powders. Studies have shown the importance of structure and morphology has on the properties of ZnO, therefore a complete understanding of the formation mechanism is needed to tailor the properties of the ZnO to specific applications [5, 40]. At present, the ZnO formation process occurring in the low-temperature hydrothermal process is not fully understood and further studies are required to fully explain the growth mechanisms behind the oxide structures and morphologies on the various substrates.

4. Conclusion

Crystalline ZnO powders with different structures and morphologies, both at the nanometre and micrometre scales have been successfully produced using a convenient low-temperature hydrothermal method. The synthesis of the ZnO powders was carried out at 90 ºC using conventional laboratory equipment such as a hotplate fitted with a magnetic stirrer and glassware. Each substrate type was able to produce a different variety of morphologies ranging from rods to flower-like structures. The low-temperature hydrothermal method uses conventional laboratory equipment and is economical. However, further studies are needed to investigate the formation mechanism behind the growth of the various ZnO forms on the different substrate types.

Acknowledgements

The authors would like to thank Dr Zhong-Tao Jiang and Ms. Xuan Le for her assistance with the FESEM imaging and both Ms Xuan Le and Mr. Tim Thomson for their assistance in the laboratory work.

Disclosure

The authors report no conflict of interest in this work.

References

[1] Yi, G. C., Wang, C. and Park, W. I. ZnO nanorods: synthesis, characterization and applications. *Semicond. Sci. Technol.*, 2005; 20: 22-34.
[2] Wang, Z. L. Zinc oxide nanostructures: growth, properties and applications. *J. Phys.: Condens. Matter*, 2004; 16: R829–R858.
[3] Singh, D. P. Synthesis and Growth of ZnO Nanowires. *Science of Advanced Materials*, 2010; 2: 245–272.
[4] Inoue, Y., Okamoto, M., Kawahara, T. and Morimoto, J. Superimposed emissions on enhanced green emission from ZnO:Pr powders by evacuated sealed silica tube method, *J. Alloys Compd.* 2006; 40: 1234–1237.
[5] Zhang, Y., Ram, Y. K., Stefanakos, E. K., and Goswami, D. Y. Synthesis, Characterization, and Applications of ZnO Nanowires. *Journal of Nanomaterials*, Volume 2012, Article ID 624520, 1-22.
[6] Zhao, F., Li, X., Zheng, J., Yang, X., et al. ZnO pine-nanotree arrays grown from facile metal chemical corrosion and oxidation, *Chem. Mater*, 2008; 20: 1197–1199.
[7] Calhoun, M. F., Sanchez, J., Olaya, D., Gershenson, M. E., et al. Electronic functionalization of the surface of organic semiconductors with self-assembled monolayers, *Nat.*

Mater, 2008; 7: 84–89.
[8] Zhou, J., Xu, N. and Wang, Z. L. Dissolving behaviour and stability of ZnO wires in biofluids: a study on biodegradability and biocompatibility of ZnO nanostructures. *Advanced Materials*, 2006; 18(18): 2432–2435.
[9] Taccola, L., Raffa, V., Riggio, C., Vittorio, O., Lorio, M. C., et al. Zinc oxide nanoparticles as selective killers of proliferating cells. *International Journal of Nanomedicine*, 2011; 6: 1129-1140.
[10] Rasmussen, J. W., Martinez, E., Louka, P. and Wingett, D. G. Zinc oxide nanoparticles for selective destruction of tumor cells and potential for drug delivery applications. *Expert. Opin. Drug Deliv*, 2010; 7(9): 1063-1077.
[11] Tseng Y. K, Huang, C. J, Cheng, H. M., Lin, I. N., et al. *Characterization and field emission properties of needle-like Zinc Oxide nanowires grown vertically on conductive Zinc Oxide films. Advanced functional materials*, 2003; 13(10) 811-814.
[12] Yi, G. C, Wang, C. and Park, W. ZnO nanorods: synthesis, characterization and applications. *Semicond. Sci. Technol*., 2005; 20: 22-34.
[13] Fan, Z.Y. and Lu, J. G. Electrical property of ZnO nanowires characterized by a scanning probe, *Appl. Phys. Lett.*, 2005; 86: 032111–032113.
[14] Lin, Z. X., Guo, T. L., Hu, L. Q., Yao, L.,J.J. Wang, J. J., et al. Tetrapod-like ZnO nanostructures serving as cold cathodes for flat-panel displays. *Acta Phys. Sin*., 2006; 55: 5531–5534.
[15] Martinson, A. B. F., Elam, J. W., Hupp, J. T. and Pellin, M. J. ZnO nanotube based dye sensitized solar cells, *Nano Lett.*, 2007; 7: 2183–2187.
[16] Wang, Z. L. Nanostructures of zinc oxide. *Materials Today*, 2004; 7(6) 26-33.
[17] Gimenez, A. J., Yá˜nez-Limón, J. M. and Seminario, J. M. ZnO-paper based photoconductive UV sensor, *J. Phys. Chem. C*, 2011; 115: 282–287.
[18] Falconi, C., D'Amico, A., and Wang, Z. L. Wireless Joule nano-heaters. *Sensors and Actuators B: Chemical*, 2007; 127(1): 54-62.
[19] Gao, P. X. and Wang, Z. L. Nanoarchitectures of semiconducting and piezoelectric zinc oxide. *Journal of Applied Physics*, 2005; 97: 1-7.
[20] Wang, Z.L. and Song, J. H. Piezoelectric Nanogenerators Based on Zinc Oxide Nanowire Arrays. *Science*, 2006; 312: 242-246.
[21] Kanade, K. G., Kale, B. B., Aiyer, R. C. and Das, B. K. Effect of solvents on the synthesis of nano-size zinc oxide and its properties. *Materials Research Bulletin*, 2006; 41: 590-600.
[22] Xu, C. X., Sun, X. W., Dong, Z. L., Yu, M. B., Xiong, Y. Z. Chen, J. S. Magnetic nanobelts of iron-doped zinc oxide. *Applied Physics Letters*, 2005; 86: 1-3.
[23] Zhao, M. H., Wang, Z. L., and Mao, S. X., Piezoelectric Characterization of Individual Zinc Oxide Nanobelt Probed by Piezo-response Force Microscope. *Nano Letters*, 2004; 4(4): 587-890.
[24] Raula, M., Rashid, M.H., Paira, T. K., Dinda, E., Mandal, T. K. Ascorbate-assisted growth of hierarchical zno nanostructures: sphere, spindle, and flower and their catalytic properties, Langmuir 2010; 26: 8769–8782.
[25] Sarkar, S. and Basak, D. Synthesis of dense intersecting branched tree-like ZnO nanostructures and its superior LPG sensing property. *Sensors and Actuators B: Chemical*, 2013; 176: 374-378.
[26] Wang, Z. Q., Liu, X. D.,Gong, J. F.,Huang, H. B., Gu, S. L.,Yang, S. G. Epitaxial growth of ZnO nanowires on ZnS nanobelts by metal organic chemical vapor deposition, *Cryst. Growth Des*, 2008; 8: 3911–3913.
[27] Daragh, B., Rabie, F. A., Teresa, B., David, G. R., Brendan, T., et al. Study of morphological and related properties of aligned zinc oxide nanorods grown by vapour phase transport on chemical bath deposited buffer layers, *Cryst. Growth Des*, 2011; 11: 5378–5386.
[28] Cheng, J. P., Zhang, X. B., Tao, X. Y., Lu, H. M., et al. Fine-tuning the synthesis of ZnO nanostructures by an alcohol thermal process, *J. Phys. Chem. B*, 2006; 110: 10348–10353.
[29] Hong, J., Choi, J., Jang, S. S., Gu, J., Chang, Y., et al. Magnetism in dopant-free ZnO nanoplates, *Nano Lett*, 2012; 12: 576–581.
[30] Gao, P. X., Mai, W. J., Wang, Z. L. Superelasticity and nanofracture mechanics of ZnO nanohelices, *Nano Lett*, 2006; 6: 2536–2543.
[31] Zhao, F. H., Lin, W. J., Wu, M. M., Xu, N. S., et al. Hexagonal and prismatic nanowalled ZnO microboxes, *Inorg. Chem*, 2006; 45: 3256–3260.
[32] Li, S., Li, Z. W., Tay, Y. Y., Armellin, J., Gao, W. Growth mechanism and photonic behaviours of nanoporous ZnO microcheerios, *Cryst. Growth Des*, 2008; 8: 1623– 1627.
[33] Li, C., Fang, G. J., Su, F. H., Li, G. H., et al. Self-organized ZnO microcombs with cuboid nanobranches by simple thermal evaporation, Cryst. Growth Des, 2006; 6: 2588–2591.
[34] Shi, R., Yang, P., Dong, X., Ma, Q., Zhang, A. Growth of flower-like ZnO on ZnO nanorod arrays created on zinc substrate through low-temperature hydrothermal synthesis. *Applied Surface Science*, 2013; 264: 162– 170.
[35] Wu, C. C., Wu, D. S., Lin, P.R., Chen, T. N., Horng, R. H. Three-step growth of well-aligned ZnO nanotube arrays by self-catalyzed metal organic chemical vapour deposition method, *Cryst. Growth. Des*, 2009; 9: 4555–4561.
[36] Protasova, L. N., Rebrov, E. V., Choy, K. L., et al., ZnO based nanowires grown by chemical vapour deposition for selective hydrogenation of acetylene alcohols, *Catalysis Science and Technology*, 2011; 1(5): 768–777.
[37] Petersen, E. W., Likovich, E. M., Russell, K. J., and Narayanamurti, V. Growth of ZnO nanowires catalyzed by size-dependent melting of Au nanoparticles, *Nanotechnology*, 2009; 20(40): Article ID 405603.
[38] Byrne, D., McGlynn, E., Kumar, K., Biswas, M., Henry, M. O., Hughes, G. Study of drop-coated and chemical bath-deposited buffer layers for vapor phase deposition of large area, aligned, zinc oxide nanorod arrays, *Cryst. Growth Des*, 2010; 10: 2400– 2408.
[39] Wang, L., Zhang, X., Zhao, S., Zhou, G., Zhou, Y., and Qi, J. Synthesis of well- aligned ZnO nanowires by simple physical vapour deposition on c-oriented ZnO thin films without catalysts or additives, *Applied Physics Letters*, 2005; 86(2): Article ID 024108.
[40] Tian, Z.R., et al., Complex and oriented ZnO nanostructures. *Nature Materials*, 2003; 2: 821-826.
[41] Sugunan, A., Warad, H. C., Boman, M. and Dutta, J. Zinc oxide nanowires in chemical bath on seeded substrates: role of hexamine. *Journal of Sol-Gel Science and Technology*, 2006; 39(1): 49–56.
[42] Lu, C. Y., Chang, S. J., Chang, S. P., et al., Ultraviolet photodetectors with ZnO nanowires prepared on ZnO:Ga/glass templates, *Applied Physics Letters*, 2006; 89(15): Article ID 153101.
[43] Lu, C. Y., Chang, S. P., Chang, S. J., et al., A lateral ZnO nanowire UV photodetector prepared on a ZnO:Ga/glass template, *Semiconductor Science and Technology*, 2009; 24(7): Article ID 075005.
[44] Kim, J. Y., Cho, J. W., and Kim, S. H. The characteristic of the ZnO nanowire morphology grown by the hydrothermal method on various surface-treated seed layers, *Materials Letters*, 2011; 65(8): 1161–1164.
[45] Jiaqiang, X., Yuping, C., Daoyong, C., and Jianian S. Hydrothermal synthesis and gas sensing characters of ZnO nanorods, *Sensors and Actuators B*, 2006; 113: 526-531.
[46] Song, J., Baek, S., Lee, H. and Lim, S. Selective growth of vertical ZnO nanowires with the control of hydrothermal synthesis and nano-imprint technology, *Journal of Nanoscience and Nanotechnology*, 2009; 9(6): 3909–3913.